EUROPEAN ORGANIZATION FOR NUCLEAR RESEARCH

CERN PPE/95-34
2 March 1995

Recent Precision Electroweak results from LEP

M. Koratzinos *

Abstract

An overview of electroweak physics with emphasis on recent results from LEP is presented. The combination of high statistics and accurate energy determination during the 1993 LEP scan improve the accuracy on nearly all electroweak observables by significant amounts. Despite this increased accuracy, the agreement of the data and the Standard Model predictions is remarkable. The pure electroweak part of the theory is seen for the first time, since data are now accurate enough to show a deviation from the pure QED radiative corrections. Standard model fits constrain the mass of the top to a narrow range around 170 GeV. Confirmation of the recent evidence for top quark production will start to constrain the mass of the Higgs, albeit weakly.

Invited talk at
The Workshop on Perspectives in Theoretical
and Experimental Particle Physics,
Trieste 7-8 July 1994.

Geneva, Switzerland

*CERN, Geneva.

1 Introduction

1.1 The Large Electron - Positron collider (LEP)

LEP is currently the world's largest accelerator. It is housed in a 27 km long underground tunnel at CERN, near Geneva. During the first phase of LEP (1989 to 1995), the centre of mass energy of the electron-positron collisions is designed to be close to the Z^0 boson mass. The Z^0 resonance increases the e^+e^- cross section dramatically (an increase of $few \times 10^2$ over the TRISTAN energies for example) to a hadronic cross section of about $30nb$ at the Z^0 peak. Most of the Z^0s created at LEP decay into hadrons (with a branching fraction of about 70%), whereas the branching fraction of Z^0 to charged leptons is about 10%. The remaining 20% of the time the Z^0 decays into a neutrino-antineutrino pair, leaving no visible traces in the detectors.

Four general purpose experiments are built at four interaction regions around the LEP ring, each a collaboration of hundreds of physicists. The number of events collected by each experiment varies from year to year depending on running conditions, but to give a feeling about overall statistics, LEP produces on average about one million Z^0s per experiment per year. The existence of four experiments working on a common wide physics field goes much further than the obvious benefit of having four times the statistics when combining all LEP data: The close collaboration of the four experiments needed when combining the LEP measurements and the necessary evaluation of each other's results, ensures a high level of quality in the overall LEP physics outcome.

1.2 Physics motivation

The theory describing our current understanding of particle physics, referred to as the Standard Model, uses a set of assumptions and some input parameters to derive predictions on all observables. Therefore, a set of accurate measurements can probe the Standard Model assumptions and measure or set limits to some of the (unknown) input parameters of the model. LEP's ability to provide a set of exceptionally accurate measurements makes it a very important tool for probing the Standard Model.

1.3 Data set used

In this report, I have used all available data up to and including 1993. All results presented here that include 1993 data are preliminary. The data and fitted parameter values shown are the ones presented in the 1994 winter conferences [1] [2] [3], with the exception of the top search data (which were not available in March '94).

2 The Standard Model

The Standard Model, the theory that contains our current understanding of nature but which does not attempt to describe it at energies well above what is available to current accelerators, is a very successful theory, although from the theoretical point of view is intuitively uncomfortable, mainly due to its large number of assumptions and input parameters

that seem rather arbitrary. Years of confrontation with experimental data of ever increasing accuracy, however, have left the Standard Model largely intact.

The input values for the Standard Model, which if known accurately can yield predictions on all observables, are the following:

- The number of fermion families, measured already at LEP in 1989 to be equal to three.
- The (nine) fermion masses - The most important unknown here is the value of the mass of the top quark, whose existence is still to be confirmed experimentally.
- Four CKM mixing matrix elements.
- One Higgs mass.
- Four parameters to determine all gauge boson masses and couplings to fermions. These are normally given as: α_{EM}, known to a precision of about 5×10^{-8} from the electron charge; G_F known to an accuracy of about 10^{-5} from muon decay; M_Z known to an accuracy of 6×10^{-5} from LEP data taken before 1993; and α_s, known to a 5% accuracy (again from LEP data).

One important postulate of the Standard Model is lepton universality - the assumption that all lepton species are equivalent. This, again according to LEP data, has been seen to be true at the 1% level.

The LEP physics programme can contribute to our knowledge of the Standard Model by increasing the accuracy of some of the input values to the Standard Model and test its assumptions; more specifically LEP can improve on the accuracy of M_Z, α_s, can check universality to higher accuracies, and can put limits on the mass of the top and the mass of the Higgs. This is done by fitting the LEP data with the Standard Model predictions and minimizing with respect to the Standard Model's input parameters.

3 Fundamental processes at LEP

At LEP, electrons and positrons interact at a centre-of-mass energy close to the Z^0 peak, giving a fermion antifermion pair: $e^+e^- \rightarrow f\bar{f}$. At these energies, the dominant process is that of Z^0 exchange. In the special case of f=e the situation is slightly more complicated due to the presence of t exchange diagrams. To lowest order the cross sections are given by:

$$\sigma_{f\bar{f}}(s) = \sigma^0_{f\bar{f}} \frac{s\Gamma_Z^2}{(s - M_Z^2)^2 + M_Z^2\Gamma_Z^2} \; + \; \gamma \; terms \; + \; \gamma Z^0 \; terms \qquad (f \neq e) \qquad (1)$$

where

$$\sigma^0_{f\bar{f}} = \frac{12\pi}{M_Z^2} \frac{\Gamma_{ee}\Gamma_{f\bar{f}}}{\Gamma_Z^2} \qquad (2)$$

The observed cross section, however, results from a convolution of the theoretical cross section with a (rather involved) function that accounts for the effect of radiative corrections. These corrections are large compared to the experimental precision and it is through virtual radiative corrections that the cross sections measured at LEP are sensitive to masses that are beyond the energy scale of LEP, such as the mass of the top quark. The biggest contribution to radiative corrections comes from initial state photon radiation, which modifies the $\sqrt{s}$

of the event. Modifications to the propagator (vacuum polarization) and final state QCD corrections (for instance gluon emission) also give sizable effects.

The differential cross section with respect to the cosine of the angle of the positron and the antifermion is proportional to

$$\frac{d\sigma_{f\bar{f}}}{d(cos\theta)} \propto 1 + cos^2\theta + \frac{8}{3}A_{FB}cos\theta \tag{3}$$

where A_{FB} is the forward-backward asymmetry ($= \frac{N_F - N_B}{N_F + N_B}$). In the Standard Model, the partial widths and the forward-backward asymmetries can be expressed as a function of the vector and axial vector coupling constants of the neutral current to fermions, g_V and g_A.

$$\Gamma_{f\bar{f}} = \frac{G_F M_Z^3}{6\pi\sqrt{2}} \left[(g_A^f)^2 + (g_V^f)^2 \right] \tag{4}$$

and

$$A_{FB}^f = \frac{3}{4} A_e A_f \qquad where \qquad A_f = \frac{2 g_V^f g_A^f}{(g_V^f)^2 + (g_A^f)^2} \tag{5}$$

A convenient way to parametrise the effect of virtual radiative corrections, so that different measurements can be easily compared, is to define the *effective* weak mixing angle

$$sin^2\theta_{eff} = \frac{1}{4}\left(1 - \frac{g_V}{g_A}\right) \tag{6}$$

3.1 LEP observables

The LEP experiments use standard Electroweak libraries [4] [5] to compute the theoretical expectations for lineshape parameters. The results can be expressed in many ways, but the parameter set commonly adopted is M_Z, Γ_Z, σ_h^0, R_l, and $A_{FB}^{0,l}$, since these parameters have minimal correlations amongst them and hence the averaging procedure of all four experiments is more transparent. The above 9-parameter set can be reduced to a 5-parameter set with the extra assumption of lepton universality.

Tau polarization analysis yields two important observables, A_τ and A_e, whereas the heavy flavour analysis yields results for b and c quark production ratios and asymmetries: $R_b (= \Gamma_{b\bar{b}}/\Gamma_h)$, $R_c (= \Gamma_{c\bar{c}}/\Gamma_h)$, $A_{FB}^{0,b}$ and $A_{FB}^{0,c}$. Finally, the $q\bar{q}$ charge asymmetry, Q_{FB} completes the picture of LEP observables.

4 The LEP 1993 scan

Using all available LEP data up to 1992, the errors on M_Z and Γ_Z were about 7 MeV for both quantities. A new scan was decided to be performed in 1993 with the aim of reducing the above errors by a factor of two. This large reduction in the errors would be possible if two conditions were met: Firstly, that the statistics delivered by LEP would be more than what was taken before 1993, and secondly that the LEP energy would be known at least a factor of two more accurately than before.

4.1 1993 statistics and scan strategy

The first goal of the 1993 scan was met thanks to the excellent performance of LEP during the whole year. $40\,\mathrm{pb}^{-1}$ were delivered in total per experiment with luminosities routinely exceeding LEP's design value of 1.3×10^{31} in all four interaction points. The amount of statistics delivered were more than a factor of two higher than the previous LEP scan year, 1991. Each experiment has reconstructed about 650,000 hadronic events and between 20,000 and 30,000 leptonic events in each of the electron, muon and tau channels during 1993.

The number of scan points and the amount of time spent on each was decided upon with two goals in mind: To optimize the total error on the mass and the width of the Z^0 while at the same time sacrificing the smallest amount of statistics for the rest of the LEP experimental programme. A three point scan was thus favoured (over a five or seven point scan). The peak point was chosen to be within 100-200 MeV from the Z^0 peak, compatible with good machine performance. The low energy point (referred to as 'peak-2' point) was about 1.8 GeV lower whereas the high energy point (referred to as 'peak+2') was symmetrically taken about 1.8 GeV higher than the peak. The statistics were shared equally between peak/off-peak operation and equally between peak+2/peak-2 points resulting in $10pb^{-1}$ at peak-2, $20pb^{-1}$ at peak and $10pb^{-1}$ at peak+2. To minimize the effect of possible systematic biases, the machine alternated between peak+2, peak and peak-2 energies during the whole of the scan period.

4.2 LEP energy determination

As we shall see later, the statistical error of the four experiments combined together on the mass and the width of the Z^0 is 1.8 MeV and 2.6 MeV respectively. Therefore, if one is to make efficient use of the available statistics, the energy uncertainty of LEP has to match these numbers. This is a rather stringent requirement if one recalls that the errors on the mass and width of the Z^0 due to the LEP energy uncertainty reported in the summer conferences of 1993 were 6 and 4.5 MeV respectively [6].

4.2.1 Quantities affecting the LEP energy

The mean energy of electrons and positrons circulating in the LEP ring is a function of the magnetic fields they encounter in their path.

The circulating beams move on a central orbit whose length is defined by the RF frequency, which is known to adequate precision and does not change during physics running; particles moving out of the orbit will see different RF accelerating fields than the average, which will put them back to the central orbit.

There are two categories of magnetic fields, which affect the energy of circulating beams in a different way: dipole fields and higher order fields.

Dipole fields define the bending strength of the magnets that deflect the electrons around the ring. Since the electrons are constrained to move in the orbit defined by the RF frequency, the higher the $\int Bdl$ seen by the electrons, the higher their energy should be. The quantities affecting the total dipole field seen by the electrons is the current of the main bend magnets, the hysteresis properties of these magnets, their length and the permeability constant of the material between the magnets and the beam. The last two are affected by the temperature

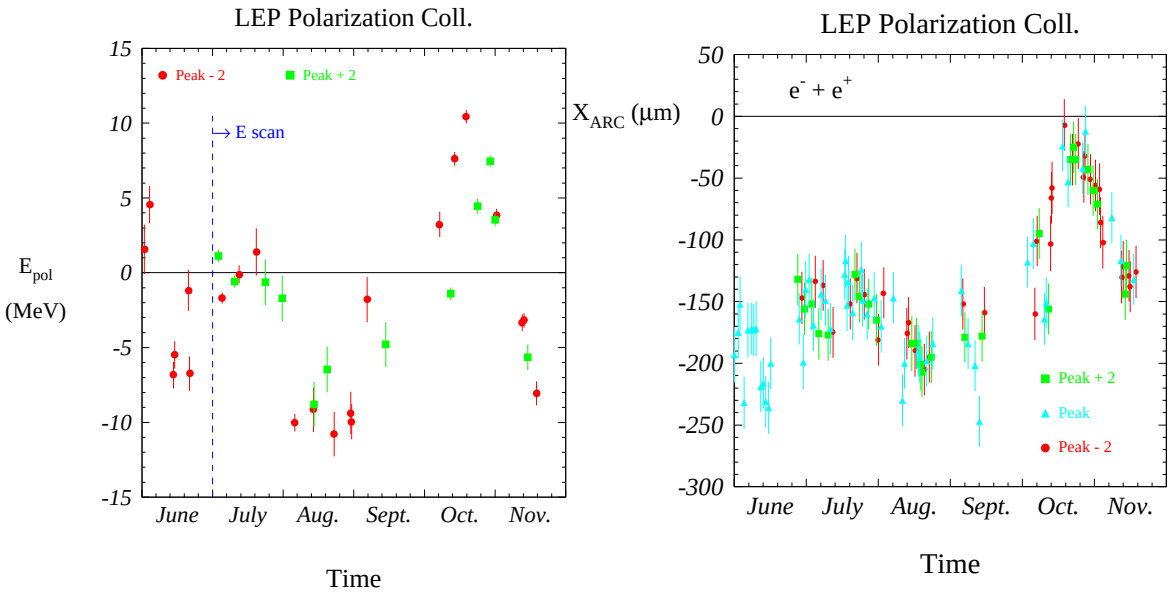

Figure 1: The left plot shows the variation of the LEP energy measurement using the resonant depolarization technique, whereas the right plot shows the mean position of the beam around the LEP arcs; 13 microns of beam displacement in the arcs corresponds to 1 MeV in beam energy. All points have been corrected for the effect of tides.

and humidity of the LEP ring. Studies have shown that if the humidity is kept at reasonable levels, its effect on the magnetic field can be neglected.

For the higher order fields (effectively quadrupole fields in our case) the situation is different; the electrons see a different field depending on the beam position with respect to the centre of the quadrupoles, and this effect dominates over small quadruple current variations. This effect produces a beam orbit - beam energy relationship, where by 'beam orbit' we denote the relative position of the beam with respect to the LEP ring. As we have seen, in absolute scale the beam orbit is constant and defined by the RF frequency, whereas the size of the LEP ring itself is influenced by geological factors, like terrestrial tides [7] and other long term variations [8] that have sizeable effects on its total length.

The centre of mass energy at each interaction point is further influenced by the RF system which is not symmetric with respect to the four LEP experiments resulting in small, calculable, differences [9].

The influence of all above factors on the LEP energy results in typical changes in the centre of mass energy of the order of 1 MeV per hour. This is of about the same magnitude as the error we are aiming to achieve, therefore the LEP energy should be monitored with a frequency larger than once per hour.

4.2.2 The strategy for minimizing the errors

The strategy for measuring the LEP energy can be summarized as follows: we are using a *model* to follow relative changes to the LEP energy, taking into account all known factors

that affect the energy of the beams. For this model to be accurate, we need careful and reliable monitoring of all quantities affecting the energy, as well as their exact relationship to energy changes.

A large monitoring operation was thus undertaken in 1993 with thousands of relevant quantities being logged at a frequency of a few per hour. The quantities mostly affecting the LEP energy were the well-known from previous years tides, the status of the RF cavities and the temperature of the magnets around the ring. Due to the success of the monitoring operation, the corrections to the LEP energy due to the above factors introduce a negligible error to the mass and the width of the Z^0 (about 0.3 MeV).

However, we are still left with two questions: We do not know the absolute scale of the energy, and we also do not know the effect of quantities that are not taken into account in our model. To solve both problems, we need an energy measurement that relies on different principles than magnetic field calculations and which is also rather accurate. A method that satisfies both criteria is the energy measurement using the technique of resonant depolarization [10]. This is a powerful method that uses the fact that in an accelerator like LEP, the number of precession turns of transversely polarized electrons, the so-called spin tune, is proportional to the mean energy of the electrons in the machine. This method measures the instantaneous energy of the machine with an accuracy better than 1 MeV. It could be performed on all three energy points in 1993, it was however expensive in terms of delivered luminosity since a measurement took about four hours with no physics data-taking possible during that time. This rather long time needed for a measurement prohibited frequent energy calibrations, and hence defined the overall strategy. A resonant depolarization measurement was routinely performed approximately twice a week during the scanning period: About 30% of all fills at both off-peak points were successfully calibrated.

Apart from the direct energy measurement, the resonant depolarization method also allows the determination of the error of our model of the LEP energy for the first time: Since the calibrated fills are an unbiased sample of all physics fills, the scatter of the difference of the energy given by the model and the energy measured with the resonant depolarization method gives the total fill to fill error due to all sources, known and unknown. We then only need to rely on assumptions and indirect measurements for the small uncertainty of the energy of LEP within a fill.

The long term stability of LEP, shown in Figure 1, showed some larger than expected scatter, of the order of 10 MeV per beam. Although it seems that this scatter was due to seasonal variations, substantiated from the fact that the horizontal orbit of LEP around the arcs, which is proportional to the LEP energy, showed good correlation and a rather smooth structure (shown also in Figure 1), the error estimate given for the winter conferences conservatively assumes that there is no underlying structure in the energy of LEP versus time, the spread of the distribution taken as the LEP energy reproducibility error. The error resulting from the above assumption together with the other (also preliminary) factors contributing to the LEP energy uncertainty propagate to 4 MeV on the mass and 3 MeV on the width of the Z^0.

It is expected that the above numbers will substantially improve when the LEP energy error analysis is finalized. *

*The final LEP errors on the mass and the width of the Z^0 were finally about 1.4 MeV and 1.5 MeV respectively (Dec '94).

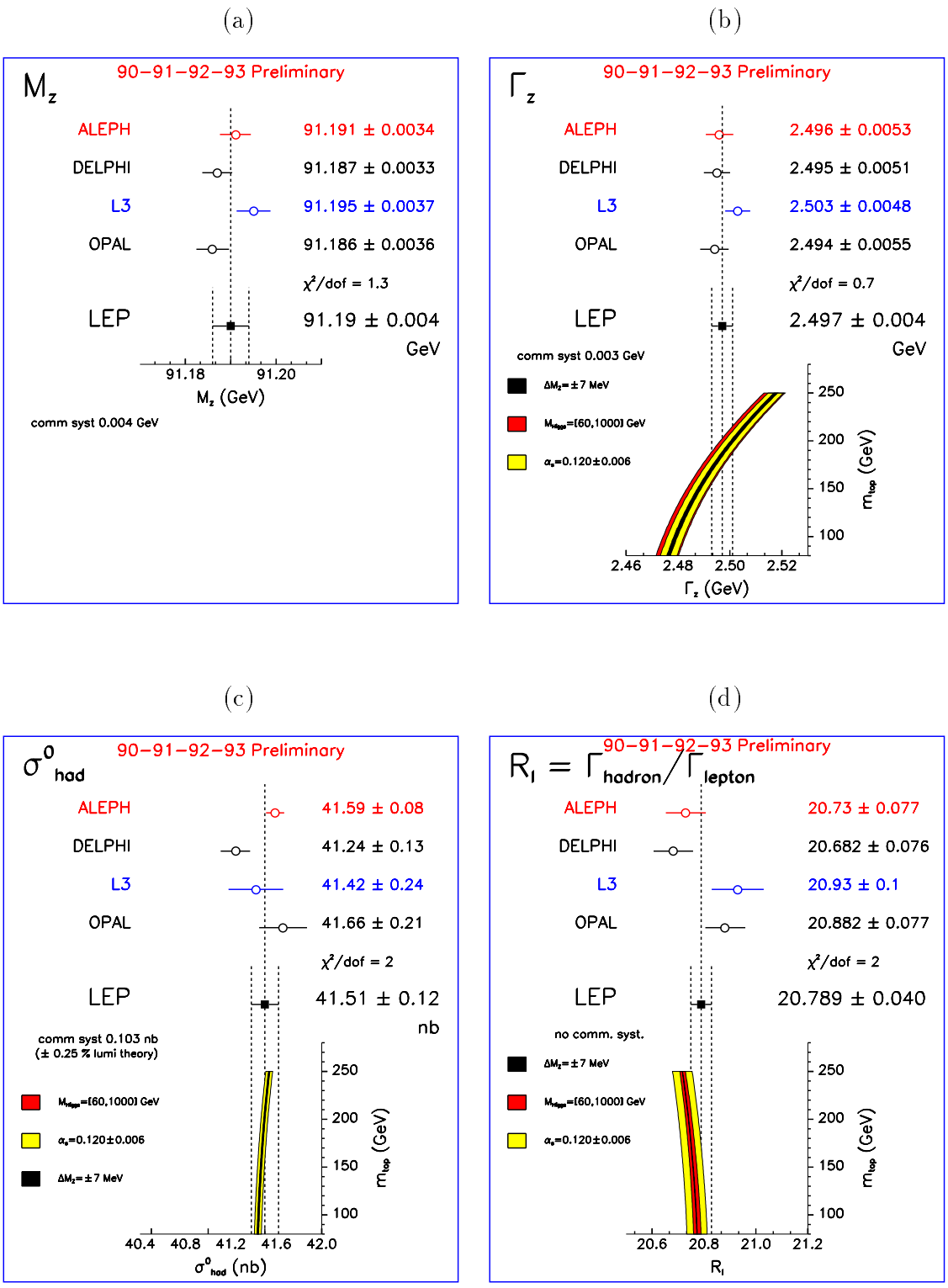

Figure 2: Experimental results and Standard Model predictions for (a) M_Z, (b) Γ_Z, (c) σ^0_{had}, and (d) R_l. The common systematic error has been subtracted from the individual experiment measurements for easier comparison of the measurements. The Standard Model predictions are shown as a function of the top quark mass.

5 Results on electroweak parameters

5.1 Mass and width of the Z^0

The determination of the mass of the Z^0, which is one of the input parameters to the Standard Model, comes effectively from the 1993 data. The results of the four LEP experiments can be seen in Figure 2(a) The agreement between the experiments is good and the average value is

$$M_Z = 91.190 \pm 0.0018 \pm 0.004(LEP) \tag{7}$$

At the moment, the preliminary beam energy (LEP) error completely dominates the combined statistical and systematic accuracy of the experiments combined.

On the Γ_Z measurement, again 1993 data dominate, the total error being reduced from about 7 MeV (summer 1993) to about 4 MeV. As is the case for the mass of the Z^0, only relative point-to-point cross sections are needed for the determination of the Z^0 width. Delphi is the only experiment to use two luminosity counters: one for relative luminosity, the other for absolute. The relative luminometer has much higher rate than the absolute luminometer, and using the information from the relative luminometer reduces the statistical error of Delphi for the mass and width of the Z^0 by about 15%. The results of the four LEP experiments can be seen in Figure 2(b). The Standard Model prediction is also shown as a function of the mass of the top quark, which has the largest influence on Γ_Z. Uncertainties due to other parameters are shown as bands in the same plot: The uncertainty on M_Z, even if taken as large as 7 MeV has a negligible effect, a 5% error on α_s and a Higgs mass varying between 60 and 1000 GeV have a slightly larger effect, even though not significant at this level of experimental precision. Combining the four experiments together one gets

$$\Gamma_Z = 2.497 \pm 0.0026 \pm 0.003(LEP) \tag{8}$$

Again, the preliminary LEP error dominates, the next important systematic error being (non-resonant) background from two photon collisions (typically about 0.5 MeV but depends strongly on hadronic Z^0 decay selection cuts).

5.2 The hadronic peak cross section

The hadronic peak cross section depends strongly on the number of light neutrinos, and in contrast to the mass and width of the Z^0, relies on absolute luminosity determination. Here, only two experiments, Aleph and Delphi, have given results for the 1993 data. Aleph claims a very low 0.09% error on absolute luminosity using their new SICAL luminometer, whereas Delphi claims a value of 0.28%, achieved however with their first generation SAT luminometer which has been replaced by a more accurate device for the 1994 data taking period. Aleph's SICAL is a state-of-the-art silicon-tungsten calorimeter build to very high precision, reaching an accuracy of 18 microns on the definition of the inner acceptance (leading to a 0.06% error on luminosity). Delphi's SAT on the other hand, relies on the mask technique to define its acceptance: A precisely machined tungsten ring with a projective outer edge is installed on the one side of the detector, sufficiently thick to stop electrons that hit it, so that a cut on the energy deposited by electrons directly translates to a cut in the inner radius. The

radius of the mask is known to a very good precision (6 microns), but the weakness of the technique lies in the fact that this very asymmetric arrangement gives strong dependence on the longitudinal position of the interaction point, which is not directly measurable by the SAT itself.

One needs to mention the impressive progress made on the luminosity front since the first yellow reports on LEP physics, where a precision of 2% was considered optimistic. However, this rapid progress on the experimental front has left the theory calculations behind: The theoretical error [11] is 0.25% and at the moment is the limiting systematic error in the determination of σ^0_{had}. There are no fundamental reasons as to why this error has to stay at such level, so a sizable reduction to the theoretical error in the near future should not come as a surprise.

The results of the four experiments can be seen in Figure 2(c) together with the LEP average and the theoretical prediction. σ^0_{had} has a small dependence on m_{top} and α_s, so that σ^0_{had} might help in α_s determination in the future.

5.3 Partial widths

The ratios of the hadronic to the leptonic partial widths (defined as $R_l = \Gamma_h/\Gamma_l$) are independent of the luminosity error. The leading systematic errors on the electron channel comes from the t-channel contribution which needs to be subtracted, resulting in a 0.2% error, and in the tau channel from the uncertainty of the acceptance (0.7%) and the two photon collision background to a smaller extent. Due to the heavy mass of the tau, its partial width differs from that of the electron and muon by about 0.23%. To be able to compare all channels in equivalent fashion, the partial width of the tau is corrected to an 'average lepton' of zero mass.

The partial widths when assuming universality and combining all lepton channels can be seen in Figure 2(d). L3 has not yet included 1993 data, whereas Delphi have only given their 'flavour blind' lepton analysis.

5.4 Lepton asymmetries

Lepton asymmetries, arising due to vector and axial vector coupling interference, together with the leptonic partial widths, are important for determining the vector and axial vector couplings (but one needs the tau polarization results to resolve relative sign and vector/axial vector ambiguities). They are derived from a fit to the $cos\theta$ distribution, which needs to be corrected for initial state radiation and QED effects, subtracting the t-channel contribution from the electron channel. The results from the four experiments can be seen in Figure 3(a) together with the Standard Model prediction (L3 has not included 1993 data in their analysis).

5.5 Tau polarization

The tau system turns out to be very important in conveying information about the ratio of coupling constants: Unlike the muon, the tau decays rather quickly and its decay products can be used to reconstruct its helicity which in turn conveys information for both A_e and A_τ.

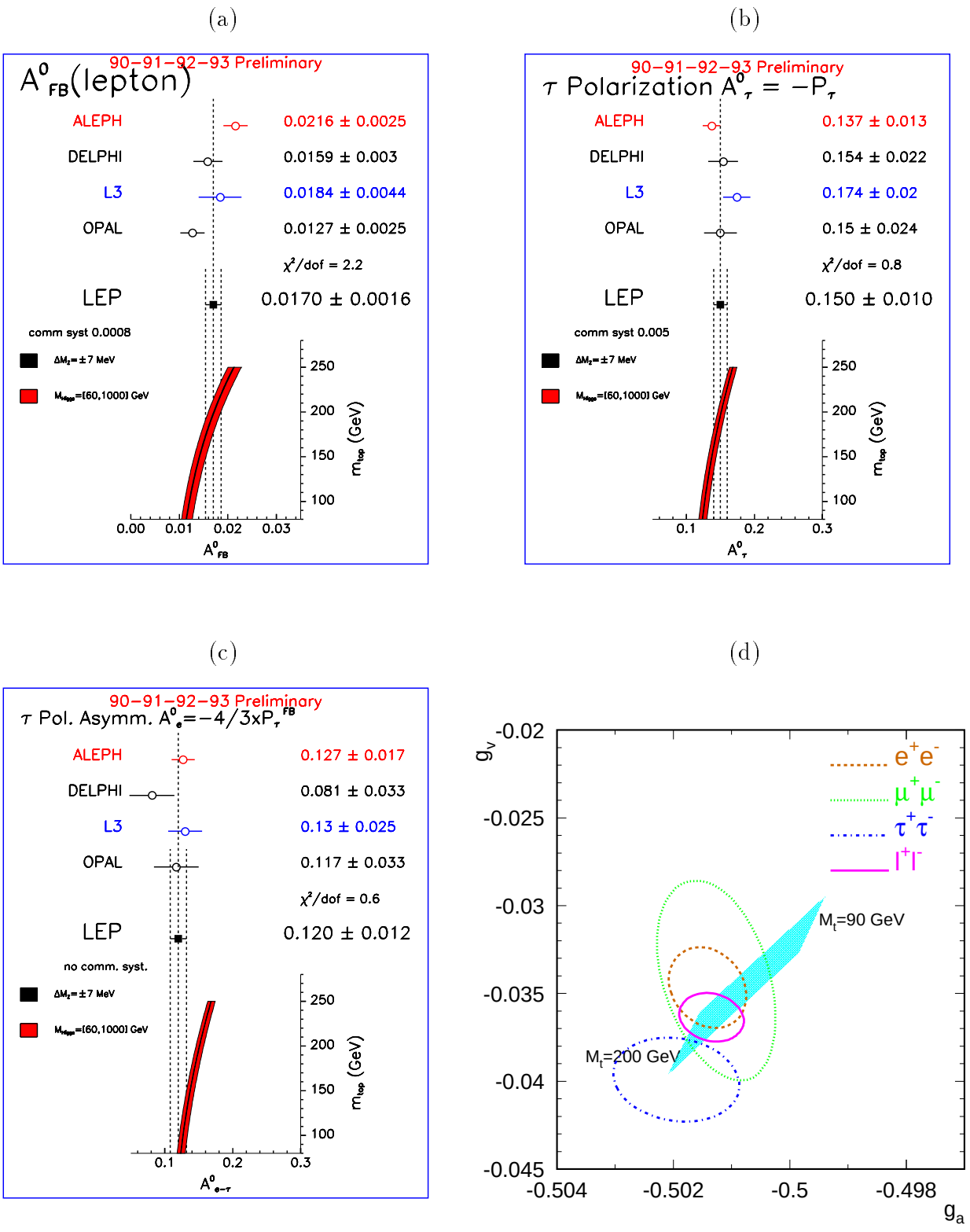

Figure 3: Experimental results and Standard Model predictions for (a) A^0_{FB}, (b) A_τ, (c) A_e, and (d) g_V versus g_A. The Standard Model predictions are shown as a function of the top quark mass. In (d) the Standard Model prediction is shown as a hatched band.

Hence it is the only process in a non-longitudinally polarized e^+e^- collider that information can be inferred on A_e without the assumption of lepton universality.

The helicity of the tau can be measured through a fit to the momentum distribution of the tau decay products. Then A_τ can be derived from the mean level of tau polarization, whereas A_e from the forward/backward asymmetry in the tau polarization. Five channels have been looked at, the highest sensitivity coming from the $\tau \to \pi\nu$ channel. Good sensitivity also comes form the $\tau \to \rho\nu$ channel, whereas the leptonic channels, although enjoying a higher branching fraction, have the presence of two neutrinos in the final state resulting in some loss of information.

The results of the four experiments on A_τ and A_e can be seen in Figure 3(b) and Figure 3(c) respectively, together with the Standard Model prediction.

5.6 Heavy flavour Electroweak results

The electroweak observables associated with heavy quarks are the ratios of the partial widths of the Z^0 decaying into $b\bar{b}$ or $c\bar{c}$, R_b and R_c, as well as the forward-backward asymmetries of b and c quarks, $A_{FB}^{b\bar{b}}$ and $A_{FB}^{c\bar{c}}$. The most interesting of these parameters is R_b; It has the special feature of depending on m_{top} but is almost insensitive to m_{Higgs}. The information of R_b is actually also contained in $R_l (= \Gamma_h/\Gamma_l)$, since one fifth of the hadronic partial width is contained in Γ_h, but it is then less significant.

Measuring R_b is a difficult experimental task, the main problem being achieving good control over heavy flavour tagging efficiency; Tagging as many heavy flavour events as possible is also difficult and a variety of tags is normally used by every experiment. Finally, averaging the results of the four LEP experiments is a tedious task that needs to be done very carefully to avoid combining results that have used different assumptions and to take properly into account all correlated uncertainties.

The most precise method of tagging events with primary b and c-quarks is the lifetime tag. Based on the relatively long lifetime of heavy quarks ($\tau_b \simeq 1.5$ps; $\tau_c \simeq 1$ps) that gives them a typical decay length of a few mm at LEP energies, this method exploits the excellent resolution of the latest generation of silicon microvertex detectors used by all LEP experiments.

The traditional method of tagging b events, the lepton tag, is also used. This method selects hadronic events with high momentum and high p_t with respect to the nearest jet axis. It is primarily sensitive to b quarks.

Finally, the event shape tag method is also used. This tries to select high statistics but rather lower purity heavy flavour events by using a complicated selection procedure based on many event shape parameters (thrust, sphericity, multiplicity, etc.). Neural network techniques are commonly used in implementing this method. Its weakness lies in the fact that it is more sensitive to imperfections of the Monte Carlo used for determining the tagging efficiency, especially in the modeling of fragmentation and decay.

Of great help to understand tagging efficiencies is the double tagging method, where one uses the extra information given by the fraction of the times where both quark and antiquark are tagged (by the same or different methods) in the same event. It is then possible to estimate the selection efficiency, including all branching fractions *and* the heavy flavour partial widths at the same time. As statistics increase, double tag methods will

dominate in determining the heavy flavour electroweak parameters.

The heavy flavour electroweak results can be seen in Table 1. Note that the values of R_b and R_c are highly correlated. R_b is about 2 standard deviations off the Standard Model prediction for an m_{top} in the vicinity of 170 GeV, but this level of disagreement does not justify any case for concern. All other quantities agree very well with Standard Model predictions

R_b	=	$0.2208 \pm 0.0013 \pm 0.0020$
R_c	=	$0.1697 \pm 0.0035 \pm 0.0134$
A^b_{FB}	=	$0.0960 \pm 0.0038 \pm 0.0021$
A^c_{FB}	=	$0.0700 \pm 0.0080 \pm 0.0072$

Table 1: Electroweak results with heavy flavour quarks.

6 Interpretation of the results

In the previous section we have presented the major new results on LEP observables. We will now deal with the interpretation of the results in the framework of the Standard Model. As it was also the case in previous years, despite the increase in accuracy of many of the measurements, none of the observables is in contradiction with what is expected by the model. The Standard Model is not yet fully constrained due to the fact that some of its ingredients have not yet been seen (the top quark and the Higgs boson), so it could be that some of its defects are currently obscured from our ignorance of the mass of the top and the mass of the Higgs. Nevertheless, the agreement between the theory and the experimental results is remarkable.

6.1 Vector and axial vector coupling constants and lepton universality

One can combine the information from the leptonic forward-backward asymmetries, the leptonic partial widths and the tau polarization to obtain values for the vector and axial vector coupling constants, g_V and g_A. A crucial postulate of the Standard model, namely that of lepton universality, can thus be tested since we have g_V and g_A information on all lepton species. The comparison of electron, muon and tau coupling constants can be seen in Figure 3(d), where the one standard deviation (39% probability) contours are plotted in the $\{g_V, g_A\}$ plane. The contour of the muon is slightly wider since it does not benefit from the tau polarization results. The agreement between all different lepton species is very good. Figure 3(d) also shows the leptonic contour, resulting from a fit assuming lepton universality.

6.2 The pure electroweak corrections

The bulk of the radiative corrections to the observables measured at LEP are of purely electromagnetic origin, therefore the general agreement of data with the Standard Model

	measurement	Standard Model fit	pull
a) LEP			
line-shape and lepton asymmetries:			
M_{Z} [GeV]	91.1895 ± 0.0044	91.192	0.6
Γ_{Z} [GeV]	2.4969 ± 0.0038	2.4967	0.1
σ^0_{h} [nb]	41.51 ± 0.12	41.44	0.6
R_ℓ	20.789 ± 0.040	20.781	0.2
$\mathrm{A}^{0,\ell}_{\mathrm{FB}}$	0.0170 ± 0.0016	0.0152	1.1
+ correlation matrix			
τ polarization:			
$\mathcal{A}_\tau$	0.150 ± 0.010	0.142	0.8
$\mathcal{A}_{\mathrm{e}}$	0.120 ± 0.012	0.142	1.8
b and c quark results:			
$R_{\mathrm{b}} = \Gamma_{\mathrm{b\overline{b}}}/\Gamma_{\mathrm{had}}$	0.2208 ± 0.0024	0.2158	2.0
$R_{\mathrm{c}} = \Gamma_{\mathrm{c\overline{c}}}/\Gamma_{\mathrm{had}}$	0.170 ± 0.014	0.172	0.1
$\mathrm{A}^{0,\mathrm{b}}_{\mathrm{FB}}$	0.0960 ± 0.0043	0.0997	0.8
$\mathrm{A}^{0,\mathrm{c}}_{\mathrm{FB}}$	0.070 ± 0.011	0.071	0.1
+ correlation matrix			
$\mathrm{q\overline{q}}$ charge asymmetry:			
$\sin^2\theta^{\mathrm{lept}}_{eff}$ from $\langle \mathrm{Q_{FB}} \rangle$	0.2320 ± 0.0016	0.2321	0.1
b) $\mathrm{p\overline{p}}$ and νN			
M_W [GeV] (CDF, CDF prel., D0 prel., UA2)	80.23 ± 0.18	80.31	0.4
$1 - M^2_{\mathrm{W}}/M^2_{\mathrm{Z}}(\nu N)$	0.2256 ± 0.0047	0.2246	0.2
c) SLC			
$\sin^2\theta^{\mathrm{lept}}_{eff}$ from $\mathcal{A}_{\mathrm{e}}$	0.2294 ± 0.0010	0.2321	2.7

Table 2: Summary of measurements included in the combined analysis of Standard Model parameters. Section a) summarizes LEP averages, section b) electroweak precision tests from hadron colliders and νN-scattering, section c) gives the result for $\sin^2\theta^{\mathrm{lept}}_{eff}$ from the measurement of the left-right polarization asymmetry at SLC. The Standard Model fit result in column 3 and the pulls in column 4 are derived from the fit including all data (Table 2, column 4) for a fixed value of $m_{\mathrm{Higgs}} = 300$ GeV.

predictions should not come as a surprise. To find out precisely how sensitive the data are to the structure of the radiative corrections in the Standard Model, and see if they agree with what is predicted, we should analyse the data in a model independent way, by writing every observable as (following [12]):

$$O_i = O_i^0 \left(1 + \sum_{j=1}^{4} a_{ij} \epsilon_j \right) \tag{9}$$

where

- O_i^0 is the corresponding prediction of the theory in the Born approximation *including* the QED radiative corrections (referred to here as the 'Born' approximation);
- ϵ_j $(j = 1, 2, 3, b)$ are four dimensionless parameters containing all the 'genuine' electroweak radiative corrections (which depend on m_{top} or m_{Higgs} or on other parameters);
- a_{ij} are fixed numerical constants.

Making reference to [12] for the exact definition of the ϵ parameters, the values we obtain from using all available data can be seen in Table 3. Three of the ϵ parameters show a 2σ deviation from zero, meaning that the data cannot be described any more by the 'Born' approximation, as was the case up to last year, and the true electroweak part is seen for the first time [13].

$\epsilon_j \times 10^3$	fit result (all data)
ϵ_1	3.0 ± 1.7
ϵ_2	-9.5 ± 5.0
ϵ_3	3.4 ± 1.8
ϵ_j	1.3 ± 4.1

Table 3: Values of the epsilon parameters using all available data. ϵ_1, ϵ_2 and ϵ_3 show a 2σ deviation from zero, the 'Born' approximation value.

6.3 Standard model fits

As we have already discussed in section 2, the Standard Model has predictions for all observables, given a set of input variables, most of which have been measured experimentally. Although to fix the model to a high degree one needs to know two more parameters, namely the masses of the top quark and the Higgs boson (whose existence has not been confirmed experimentally), one can perform a series of precision tests without this knowledge. As it can be seen from Figure 2 and Figure 3 the Standard Model predictions agree very well with the experimental data, although it is clear that if the top was found to be, for instance, very heavy (i.e. above 200-230 GeV) then the theory would have problems accommodating the results. One can turn the argument around and postulate that since the agreement with

data is generally very good, one can use the Standard Model as a predictive tool to estimate the mass of the top and the mass of the Higgs.

	LEP	LEP + Collider and ν data	LEP + Collider and ν data + $A_{\rm LR}$ from SLC
$m_{\rm top}$ (GeV)	$172^{+13\ +18}_{-14\ -20}$	$170^{+12\ +18}_{-12\ -19}$	$177^{+11\ +18}_{-11\ -19}$
$\alpha_s(M_{\rm Z}^2)$	$0.125 \pm 0.005\ \pm 0.002$	$0.125 \pm 0.005\ \pm 0.002$	$0.124 \pm 0.005\ \pm 0.002$
$\chi^2/(d.o.f.)$	11.4/9	11.5/11	19.1/12
$\sin^2\theta^{\rm lept}_{eff}$	$0.2323 \pm 0.0002\ ^{+0.0001}_{-0.0002}$	$0.2324 \pm 0.0002\ ^{+0.0001}_{-0.0002}$	$0.2320 \pm 0.0003\ ^{+0.0001}_{-0.0002}$
$1 - M_{\rm W}^2/M_{\rm Z}^2$	$0.2251 \pm 0.0015\ ^{+0.0003}_{-0.0003}$	$0.2253 \pm 0.0013\ ^{+0.0003}_{-0.0002}$	$0.2243 \pm 0.0012\ ^{+0.0003}_{-0.0002}$
$M_{\rm W}$ (GeV)	$80.28 \pm 0.08\ ^{+0.01}_{-0.02}$	$80.26 \pm 0.07\ ^{+0.01}_{-0.01}$	$80.31 \pm 0.06\ ^{+0.01}_{-0.01}$

Table 4: Results of fits to LEP and other data for $m_{\rm top}$ and $\alpha_s(M_{\rm Z}^2)$. No external constraint on $\alpha_s(M_{\rm Z}^2)$ has been imposed. In the third column also the combined data from the $\rm p\overline{p}$ experiments UA2 [15], CDF [16, 17] and D0 [17]: $M_{\rm W} = 80.22 \pm 0.16$ GeV and from the neutrino experiments, CDHS [18], CHARM [19] and CCFR [20]: $1 - M_{\rm W}^2/M_{\rm Z}^2 = 0.2256 \pm 0.0047$ are included. The fourth column gives the result when also the SLD measurement of the left-right asymmetry at SLC [14], $\sin^2\theta^{\rm lept}_{eff} = 0.2294 \pm 0.0010$, is added. The central values and the first errors quoted refer to $m_{\rm Higgs} = 300$ GeV. The second errors correspond to the variation of the central value when varying $m_{\rm Higgs}$ in the interval $60 \leq m_{\rm Higgs}\ [\rm GeV] \leq 1000$.

On doing this, one gets rather stringent limits for the mass of the top, and some, still weak at the moment, limits for the mass of the Higgs. The data used for the fits are those of Table 2. Measurements used in the fits but not reported here include the measurement of $sin^2\theta_{eff}$ coming from the measurement of A_{LR} at SLAC [14], the measurement of the W mass from $p\bar{p}$ collider experiments (UA2 [15], CDF [16] [17], and D0 [17]), and the measurement of $sin^2\theta_W$ from neutrino scattering experiments (CDHS [18], CHARM [19], and CCFR [20]). The agreement of all data is quite good, the largest contribution to the χ^2 of the fit coming from the $sin^2\theta_{eff}$ measurement of SLAC (2.7 standard deviations). The total χ^2 however is acceptable. The results for the mass of the top can be seen in Table 4 together with the fitted values for $sin^2\theta_{eff}$, $sin^2\theta_W$, and M_W. The tradition of giving the value of the top mass for a Higgs mass of 300 GeV is followed, the change in the mass of the top when the Higgs mass scans all its available range (60 to 1000 GeV) given as an extra uncertainty. Using all available data one obtains

$$m_{top} = 177^{+11\ +18}_{-11\ -19}\ (Higgs) \tag{10}$$

Figure 4 shows more clearly the predicted range of values for m_{top} and m_{Higgs}. The estimation of these masses through radiative corrections at LEP means that m_{top} is correlated to $log(m_{Higgs})$, as can be seen in the figure. Low m_{Higgs} values are preferred by the data, but the limits one can obtain to the mass of the Higgs are still not really significant.

The number of light neutrino families has been measured to be three from the first LEP scan in 1989. Small deviations from three would, however, show a deviation from the Standard Model prediction indicating new physics. Using the Standard Model formula

$$\frac{\Gamma_{inv}}{\Gamma_l} = (1.992 \pm 0.003) N_\nu \tag{11}$$

which is largely independent of the mass of the top and the mass of the Higgs, we obtain

$$N_\nu = 2.985 \pm 0.023 \tag{12}$$

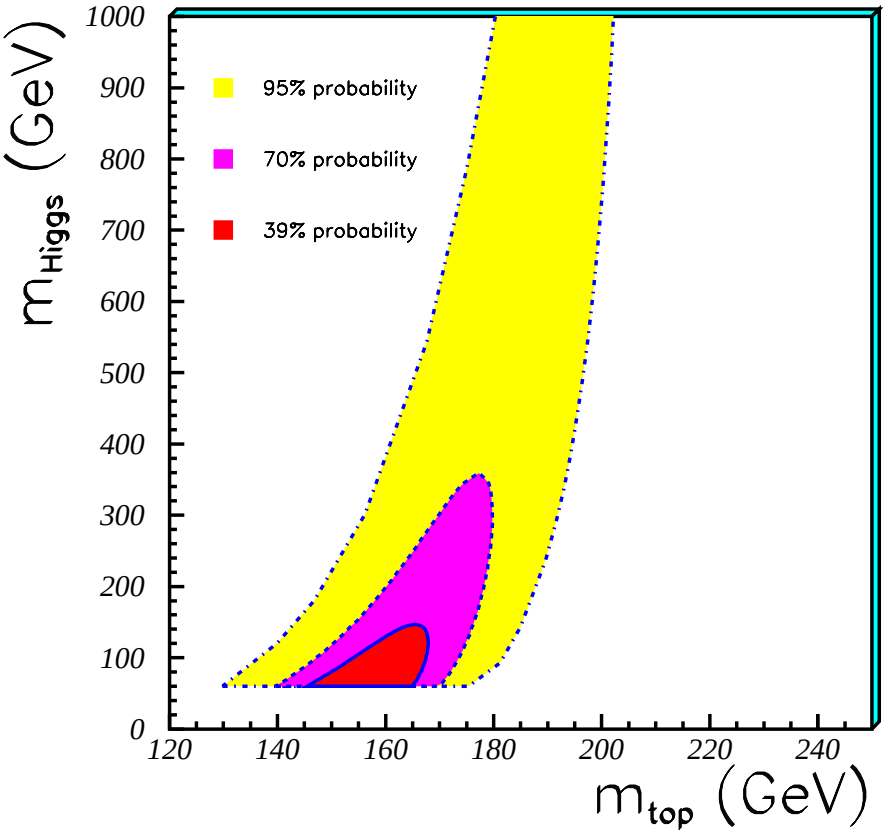

Figure 4: Standard Model fit results in the $\{ m_{top}, m_{Higgs} \}$ plane. Radiative corrections correlate m_{top} to $log(m_{Higgs})$. The straight line cut at low Higgs masses is due to the direct search Higgs limit (about 65 GeV).

α_s can be calculated through the QCD corrections affecting mainly the hadronic partial width. Using all LEP electroweak data and leaving the number of neutrinos unconstrained we obtain:

$$\alpha_s(M_Z^2) = 0.127 \pm 0.006 \pm 0.002(Higgs) \quad (N_\nu \ free) \tag{13}$$

If the number of neutrinos is fixed to three, the value changes slightly to

$$\alpha_s(M_Z^2) = 0.125 \pm 0.005 \pm 0.002(Higgs) \quad (N_\nu = 3) \tag{14}$$

The second error is again due to the Higgs mass scanning the 60-1000 GeV range. Note that this estimate of α_s is in good agreement with the value obtained from event shape measurements at LEP ($\alpha_s(M_Z^2) = 0.123 \pm 0.006$) and of similar precision, but with the advantage of being independent of fragmentation features.

The theoretical uncertainties in the above Standard Model fits are dominated by the uncertainty in the value of $\alpha_{QED}(M_Z^2)$ due to the contribution of light quarks to the vacuum polarization of the photon. An uncertainty $\delta\alpha_{QED} = 0.0009$ has been propagated in the fits.

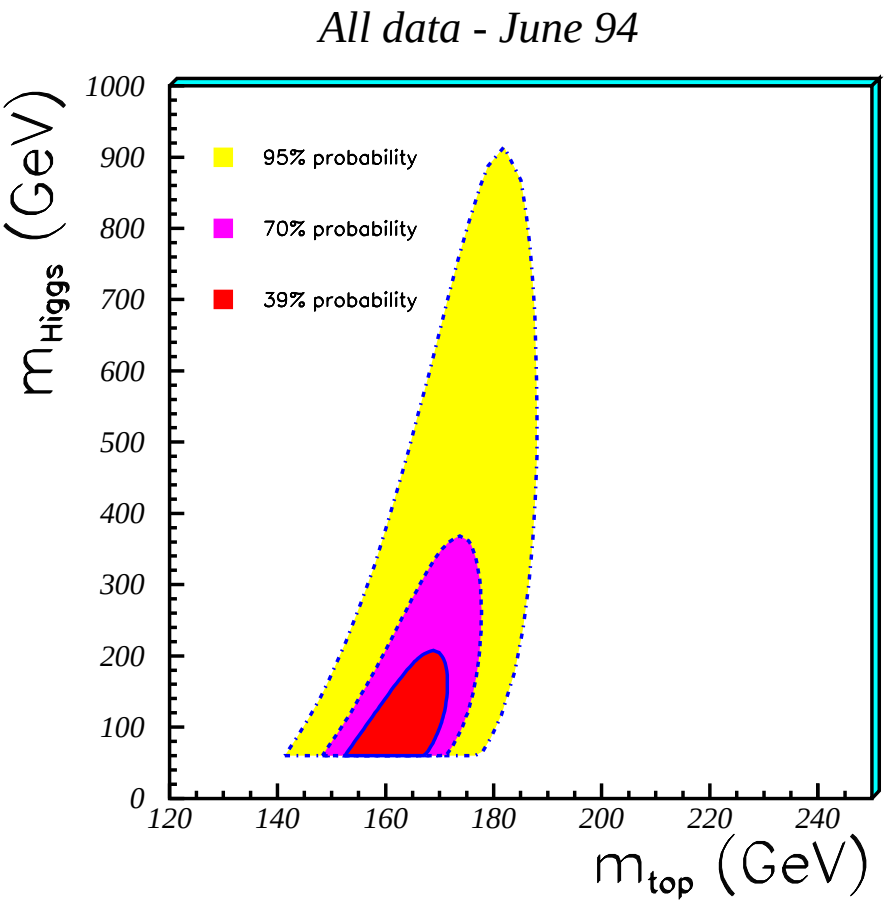

Figure 5: Standard Model fit results in the m_{top}, m_{Higgs} plane when all available data are used, including the direct search values for the mass of the top. The extra information compared to Figure 4 helps to close the 95% probability contour below 1TeV for the first time.

6.4 The mass of the Higgs

As seen from Figure 4, the available data have only just started to constrain the mass of the Higgs, and no statistically significant constraint can be established. However, we can do slightly better: A recent paper from the CDF collaboration at Fermilab [21] claims evidence for the observation of the top quark. If we assume that this evidence is true, we can use the information from the Tevatron for the mass of the top quark as an extra constraint. In this

paper we have used the Ellis et al [22] value for the combined estimate for the mass of the top of

$$m_{top} = 167 \pm 12 \ GeV \tag{15}$$

Here the direct kinematic m_{top} measurement of CDF is combined to the value obtained from the cross section seen by both CDF and D0 experiments (the value of the top mass from the direct measurement alone (from CDF) is $m_{top} = 174 \pm 16 \ GeV$). Using this value for m_{top} as an extra constraint we obtain the following for the mass of the Higgs:

$$m_{Higgs} = 50^{+100}_{-30} \ GeV \tag{16}$$

The central value coming from the fits tends to be below the direct search limit (currently at 63 GeV from LEP). The available space for the mass of the Higgs can be seen in Figure 5. [†] Although the one sigma numbers given above sound impressive, the 95% probability contour nearly touches 1TeV, so there is a long way to go before some really meaningful constraint on the mass of the Higgs is obtained. However, light Higgs masses seem to be favoured by the data, therefore we would soon need to revise our traditional policy of giving the mass of the top at a central value of the mass of the Higgs of 300 GeV. It would be more correct to quote the value of m_{top} obtained when the mass of the Higgs is left as a free parameter.

7 Conclusions

LEP is a high precision testing ground for the Standard Model. It can accurately determine fundamental variables of the Standard Model (like the mass of the Z^0) and can constrain others (like the mass of the top and, to a small extent at the moment, the mass of the Higgs.

1993 has been a tour de force of LEP that has reduced uncertainties on most measured variables by significant amounts.

Confirmation of the discovery of the top together with an accurate m_{top} measurement from direct searches can start constraining the mass of the Higgs.

The Standard Model is still going strong but will soon be running out of parameter space to hide its defects.

8 Acknowledgements

It is a pleasure to thank my colleagues at LEP, experimental physicists and machine scientists alike, who contributed to the success of the 1993 LEP campaign. I particularly wish to thank the members of the Electroweak Working Group, the body responsible for the averaging of the results, and the LEP Energy Group, responsible for delivering the LEP energies and errors, for their excellent work.

[†] Comparing Figures 4 and 5 one might think that the additional m_{top} constraint does not help in our knowledge of m_{Higgs}. This is not true as can be seen from the 95% probability contour. The fact that the 1 and 2 standard deviation contours are similar, is simply due to a statistical fluctuation that makes the χ^2 function of m_{Higgs} more narrow than expected from our precision in the case of Figure 4. The corresponding χ^2 function of Figure 5 is as expected, however.

References

[1] M. Koratzinos, *Electroweak results from LEP*, proceedings of "Les Rencontres de Physique de la Vallee d' Aoste", La Thuile, March 1994.

[2] S. De Jong, *Heavy flavour Electroweak measurements from Z^0 decays*, proceedings of "Les Rencontres de Physique de la Vallee d' Aoste", La Thuile, March 1994.

[3] The LEP Electroweak Working Group, A. Blondel et al., *Updated Parameters of the Z^0 Resonance from Combined Preliminary Data of the LEP Experiments*, ALEPH 94-74, DELPHI 94-33, L3 Note 1599, OPAL TN235.

[4] MIZA: M. Martinez et al., Z. Phys. **C49** (1991) 645.

[5] ZFITTER: D. Bardin et al., Phys. Lett. **B255** (1991) 290 and CERN-TH 6443/92 (1992).

[6] J. Lefrançois, *Precision tests of the Standard Model; The experimental results*, Rapporteur talk at the International Europhysics Conference on High Energy Physics - July 22-28, 1993, Marseille.

[7] L.Arnaudon *et al.*, *Effects of Terrestrial Tides on the LEP Beam Energy*, CERN SL/94-07 (1994).

[8] J. Wenninger, *Study of the LEP Beam Energy with Beam Orbits and Tunes*, CERN SL/94-14 (1994).

[9] G. Quast, *Uncertainties on the Energy Correction due to RF effects in 1993*, memorandum to the LEP Energy Group, 1993.

[10] L.Arnaudon *et al.*, *Accurate Determination of the LEP Beam Energy by Resonant Depolarization*, CERN SL/94-71 (1994).

[11] BHLUMI: S. Jadach et al., Comp. Phys. comm. **70** (1992) 305.

[12] G. Altarelli et al., Nucl. Phys. **B405** (1993) 3.

[13] R. Barbieri, Talk given at the Recontres de la Vallee d'Aoste, La Thuile, March 1994 and IFUP-TH 28/94 (1994).

[14] SLD Collaboration, K. Abe et al., SLAC-PUB-6456, March 1994, submitted to Phys. Rev. Lett.

[15] UA2 Collaboration, J. Alitti et al., Phys. Lett. **B276** (1992) 354.

[16] CDF Collaboration, F. Abe et al., Phys. Rev. **D43** (1991) 2070.

[17] Y. Ducros, CDF and D0 preliminary results, proceedings of "Les Rencontres de Physique de la Vallee d' Aoste", La Thuile, March 1994.

[18] CDHS Collaboration, A. Blondel et al., Z.Phys. **C45** (1990) 361.

[19] CHARM Collaboration, J.V. Allaby et al., Z. Phys. **C36** (1987) 611.

[20] CCFR Collaboration, *A Precise Measurement of the Weak Mixing Angle in Neutrino Nucleon Scattering*, NEVIS-R 1498, Submitted to Phys. Rev. Lett.

[21] CDF Collaboration, F. Abe et al., Phys. Rev. **D50** (1994) 2966.

[22] J.Ellis *et al.*, *The Top Quark and Higgs Boson Masses in the Standard Model and the MSSM*, CERN TH 7261/94 (1994).